Nuclear fission reaction simulations in compact stars

Alex Deibel [*]
Department of Astronomy, Indiana University, Bloomington, Indiana 47405, USA

M. E. Caplan [†]
Department of Physics, Illinois State University, Normal, Illinois 61790, USA

C. J. Horowitz [‡]
Department of Physics, Center for Exploration of Energy and Matter, Indiana University, Bloomington, Indiana 47405, USA

(Received 29 September 2021; accepted 27 September 2022; published 10 October 2022)

Type-Ia supernovas are powerful stellar explosions that provide important distance indicators in cosmology. Recently, we proposed a new Type-Ia supernova mechanism that involves a nuclear fission chain-reaction in an isolated white dwarf [Phys. Rev. Lett. **126**, 131101 (2021)]. Here we perform novel reaction network simulations of the actinide-rich first solids in a cooling white dwarf. The network includes neutron-capture and fission reactions on a range of U and Th isotopes with various possible values for ^{235}U enrichment. We find, for modest ^{235}U enrichments, neutron capture on ^{238}U and ^{232}Th can breed additional fissile nuclei so that a significant fraction of all U and Th nuclei may fission during the chain reaction. Finally, we compute the energy release from the fission chain reaction for various uranium enrichments; a novel result that is a necessary input for thermal diffusion simulations of carbon ignition.

DOI: 10.1103/PhysRevC.106.045803

I. INTRODUCTION

Type-Ia supernovas (SN Ia) are widely used distance indicators in cosmology [1–3], but significant tension remains between the Hubble constant determined from SN Ia and the value determined from other data [4–6]. Despite the importance of SN Ia for cosmology, their progenitor systems and explosion mechanisms are still somewhat uncertain.

Traditionally, SN Ia are thought to involve the thermonuclear explosion of a C/O white dwarf (WD) in a binary system. Here the companion is either a conventional star (single-degenerate mechanism) or another WD (double-degenerate mechanism) [7–9]. Recently we proposed an additional SN Ia mechanism that may occur in *isolated* WDs [10,11] wherein the cooling WD core rapidly precipitates a fission-critical uranium crystal within $\lesssim 30$ s. If a fission chain reaction proceeds in the crystal, it is unknown, *a priori*, the fraction of uranium consumed or the resulting energy release.

In the present paper we perform nuclear reaction network simulations of fission chain reactions in compact stars. Our goal is to determine the fraction of fissile fuel consumed during a fission chain reaction and the resulting energy release and how this depends on the uranium enrichment f_5—the fraction of all uranium that is ^{235}U. This is important input for thermal diffusion simulations of carbon ignition in an isolated WD. We present these simulations in a separate paper [12] where we find that carbon ignition is likely at high densities.

Our simulations are novel, apparently the first such calculations for a compact star. To provide context, we briefly review fission chain reactions in conventional nuclear reactors and nuclear weapons in Sec. II. Our reaction network formalism is described in Sec. III, results presented in Sec. IV, and we conclude in Sec. VI.

II. CONTEXT

A fission reaction in a compact star is a unique hybrid between a nuclear reactor and a nuclear weapon. Such as a nuclear weapon the chain reaction is expected to proceed extremely rapidly. A WD is degenerate, however, and the temperature can rise without a large increase in pressure. As a result, the system does not rapidly disassemble as in a nuclear weapon. This allows time—as in a nuclear reactor—for fertile isotopes, such as ^{238}U or ^{232}Th to capture neutrons and breed additional fissile material.

Many conventional nuclear reactors slow neutrons to (terrestrial) thermal energies to take advantage of the large fission cross section of ^{235}U at low energies. In the WD core, however, the temperature is of order ≈ 1 keV and the ^{235}U fission cross section is much smaller. Even if plenty of light nuclei are present to moderate the neutrons, the neutron energy will only be reduced to the ≈ 1-keV ambient temperature. Therefore, unlike a terrestrial nuclear reactor, a stellar system cannot take advantage of the large low-energy ^{235}U cross section.

[*] deibelalex@gmail.com
[†] mecapl1@ilstu.edu
[‡] horowit@indiana.edu

 ©2022 American Physical Society

TABLE I. Initial abundances Y_i, electron fraction Y_e, and baryon number density n_b.

U	Th	Pb	Y_e	n_b (cm^{-3})
1.3×10^{-3}	9.51×10^{-4}	2.28×10^{-3}	0.391	6.02×10^{31}

Terrestrial nuclear weapons, on the other hand, disassemble extremely rapidly because of the large energy release. This necessitates using fast neutrons in the chain reaction because slow neutrons simply take too long to cause additional fissions. By the time a slow neutron arrives to cause another fission the fuel may have been blown apart. This reliance on fast neutrons requires the use of highly enriched uranium or plutonium in a nuclear weapon.

The necessary uranium enrichment may be reduced if it is possible for the chain reaction to breed additional fissile nuclei. For example ^{238}U in a nuclear reactor can capture a neutron to become ^{239}U that, in turn, β decays twice to produce ^{239}Pu. Therefore, a fission chain reaction in a star could breed some of its nuclear fuel as the reaction progresses.

We now begin our paper by discussing the composition of the first solids to form as a WD cools. Next, we list the fission and neutron-capture reactions that are included in our network simulations and present the results for composition and energy release as a function of time. We end with a discussion of sensitivity to uranium enrichment and to the ^{238}U fission cross section. We conclude that for modest enrichments a large fraction of the available fuel is expected for fission producing a large energy release that could ignite carbon burning.

III. FORMALISM

Initial abundances. The composition of the first solids to form as material in a WD just starts to crystallize has been studied using free-energy models and with molecular dynamics simulations [10,11]. The material is U and Th rich since these elements have the highest charge Z. In addition some Pb is present because the solar system abundance of Pb is 100 times that of U. The initial abundance in nuclei per baryon $Y_i = n_i/n_b$ are listed in Table I. Here n_i is the number density of species i, and n_b is the baryon density.

In addition to heavy nuclei, some C and O may be present in the first solids. Elastic scattering from the light C and O nuclei can lower the energy of fission neutrons. At this time the amount of C and O is uncertain and may be zero. For simplicity in this first paper, we assume there is no C and O present. As a result there will be little moderation of the initial neutron energies. The fission spectrum has a most probable energy near $\approx$1 MeV. In this paper we simply assume all neutrons have an energy of 1 MeV and evaluate all cross sections at this energy. This assumption of monoenergetic neutrons greatly simplifies thermally averaged reaction rates that are proportional to the cross section times the relative velocity,

$$\langle \sigma(E)v \rangle \approx \sigma(1\ \mathrm{MeV})v_0, \tag{1}$$

TABLE II. Cross sections for neutron absorption (n, γ) and fission reactions for 1-MeV neutrons on Th and U isotopes. Also listed is the average number of neutrons emitted per fission $\bar{\nu}$. Data from Ref. [13].

Isotope	$\sigma_{n,\gamma}$ (b)	σ_f (b)	$\bar{\nu}$
^{232}Th	0.14	0.0013	2.18
^{233}Th	0.068	0.094	2.69
^{235}U	0.11	1.20	2.53
^{236}U	0.17	0.36	2.49
^{237}U	0.082	0.68	2.57
^{238}U	0.13	0.014	2.69
^{239}U	0.097	0.38	2.91
^{240}U	0.086	0.007	2.69
^{241}U	0.17	0.24	2.88

with v_0 the velocity of a 1-MeV neutron. Furthermore, this thermal average is independent of temperature.

We consider neutron-capture (n, γ) and neutron-induced fission reactions on the U and Th isotopes. We use 1-MeV cross sections from the ENDF 2011 data set available at the National Nuclear Data Center [13], see Table II. Our reaction network has ^{232}Th, ^{233}Th, and ^{234}Th isotopes and U isotopes from ^{235}U to ^{242}U. In addition we have neutrons and fission fragments. We do not distinguish different possible fission fragments and simply assume that any fission will produce two fragments. Our network has a total of 13 species consisting of three Th isotopes, eight U isotopes, n and fission fragments.

There are simple equations for the change in abundance dY_i/dt from a given reaction [14]. For example, the change in neutron abundance Y_n from the fission of nucleus A of abundance Y_A is

$$\frac{dY_n}{dt} = (\bar{\nu} - 1) n_b \sigma_f v_0 Y_n Y_A. \tag{2}$$

Here each fission produces an average number of neutrons $\bar{\nu}$ (see Table II, and one neutron was absorbed to cause the fission). The fission also increases the abundance of fission fragments Y_{ff} where we include a factor of 2 for the two fragments,

$$\frac{dY_{\mathrm{ff}}}{dt} = 2 n_b \sigma_f v_0 Y_n Y_A. \tag{3}$$

Likewise neutron absorption on nucleus A decreases its abundance and increases the abundance of nucleus $A + 1$,

$$\frac{dY_{A+1}}{dt} = -\frac{dY_A}{dt} = n_b \sigma_{n,\gamma} v_0 Y_n Y_A. \tag{4}$$

We sum terms with these forms over all of the (n, γ) and fission reactions in Table II.

The initial abundance of ^{235}U is $f_5 Y_u$ with Y_u the uranium abundance from Table I and f_5 the uranium enrichment. Likewise the ^{238}U abundance is $Y_u(1 - f_5)$. Finally for the initial neutron abundance one can use any small seed value. The cases explored are listed in Table III.

The energy released per fission is about 200 or 100 MeV per fission fragment. Therefore, the heating rate in MeV per

TABLE III. Four cases of enrichment f_5, fission cross section of ^{238}U, and neutron absorption cross section of fission fragments $\sigma_{\rm ff}$. Also listed are the initial n abundance Y_n, the fission heating S, the fraction of U and Th that fission and the final temperature T_f.

Case	f_5	$\sigma_f(^{238}\mathrm{U})$ (b)	$\sigma_{\rm ff}$ (b)	Y_n	S (MeV/A)	U %	Th %	T_f 10^9 K
A	0.14	0.014	0	10^{-9}	0.026	9.6	0.4	1.6
B	0.14	0.04	0	10^{-6}	0.358	95	58	5.9
C	0.20	0.014	0	10^{-6}	0.356	94	58	5.9
D	0.14	0.04	0.01	10^{-6}	0.325	89	49	5.6

baryon per time is

$$\dot{S} = (100\ \mathrm{MeV}) dY_{\rm ff}/dt, \tag{5}$$

and the total energy released by a time $t_{\rm final}$ in MeV per baryon is

$$S = (100\ \mathrm{MeV}) Y_{\rm ff}(t_{\rm final}). \tag{6}$$

The large fission energy release will raise the temperature of the system. We assume the reaction proceeds at constant pressure. Previously we calculated the heat capacity at constant pressure and obtained the final temperature T_f [11],

$$T_f \approx \left(\frac{8\epsilon_F S}{5\pi^2 Y_e}\right)^{1/2}. \tag{7}$$

Here ϵ_F is the electron Fermi energy and Y_e is the electron fraction, see Table I.

IV. RESULTS

A. Abundance evolution

We now present results for three cases of enrichment and ^{238}U fission cross section as listed in Table III. In all cases the chain reaction proceeds rapidly, in less than 10^{-11} s as shown in Fig. 1. This is because of the high density of the system, the large neutron cross sections, and the high velocity of 1-MeV neutrons. In general, the reaction proceeds in two stages. In the first stage neutrons from ^{235}U fission transform or breed

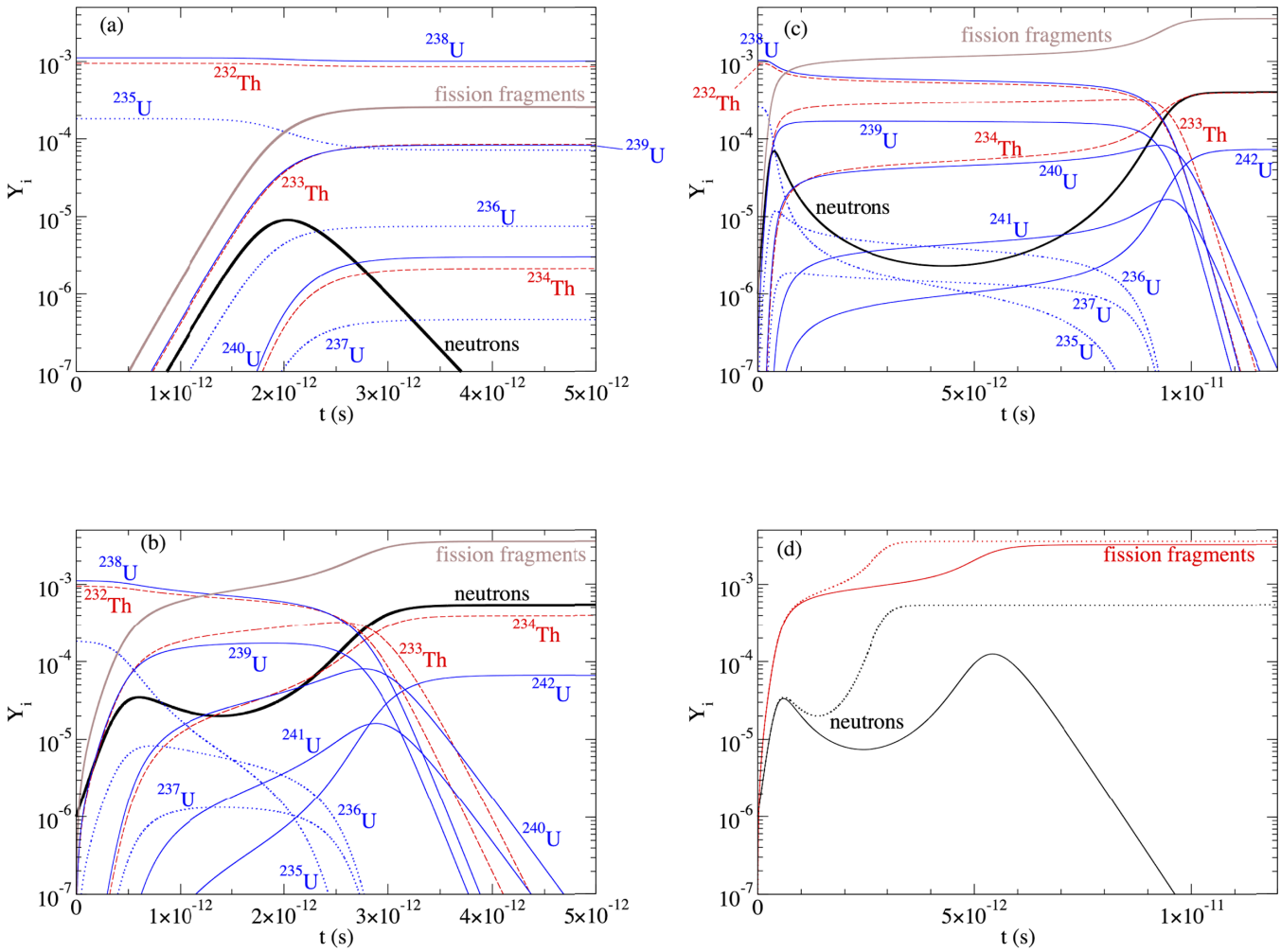

FIG. 1. Abundance per baryon Y_i versus time for Case *A* in panel (a), *B* in (b), and *C* in (c). Panel (d) shows abundance per baryon of neutrons (black curves) and fission fragments (red curves) versus time. Results are shown for Case *B* without neutron capture on fission fragments (dotted) and for Case *D* with capture (solid), see Table III.

some ^{238}U and ^{232}Th nuclei into more easily fissionable ^{239}U and ^{233}Th. In the second stage, or breeder reaction, most of the original U and a significant fraction of the Th fission.

In Case *A* we use $f_5 = 0.14$ and the unmodified 1-MeV fission cross section for ^{238}U of 0.014 b. One needs an enrichment of, at least, $f_5 \approx 0.12$ for the system to be critical. If f_5 is smaller than that no chain reaction will take place. If f_5 is only slightly larger than 0.12 we expect the chain reaction to burn a small amount of ^{235}U until the system becomes subcritical and the chain reaction stops. This will only release a small amount of fission heating.

In Fig. 1(a) we show results for Y_i versus time for Case *A*. The system fissions ≈9.6% of the total U. This includes over half of the original ^{235}U and only a small amount of ^{238}U. Only a small amount of Th fissions near ≈0.4%. We see that the neutron abundance rises exponentially with time until enough ^{235}U has been burned so that the system is no longer critical. After that Y_n decreases as the remaining neutrons are captured.

Results are very sensitive to the small ^{238}U fission cross section. This is 0.014 b at 1 MeV but rises rapidly at higher energies. A detailed calculation averaging the energy-dependent cross section over the neutron fission spectrum may give a larger value. Alternatively, as the temperature of the medium rises, ^{238}U nuclei will occupy a range of excited states, and these may have higher fission cross sections for 1-MeV neutrons. For example, Zhu and Pei calculate that the spontaneous fission half-life of ^{240}Pu decreases by 12 orders of magnitude as the temperature is increased from 0 MeV to 0.1 MeV [15]. In Case *B* we use $\sigma_f = 0.04$ b instead of 0.014 b for $\sigma_f(^{238}\mathrm{U})$. The results in Fig. 1(b) show dramatic differences from Case *A*. The reaction now proceeds in two stages. First mostly ^{235}U fissions. This releases enough neutrons so the *n* capture converts both ^{232}Th and ^{238}U into odd*A* nuclei with significant fission cross sections. In the second or breeder reaction stage these nuclei fission. As a result fully 95% of the U and 58% of the Th fissions. Note that in a terrestrial nuclear reactor there is time for ^{239}U to decay to ^{239}Pu. Here there is not enough time, and ^{239}U instead can be used directly as a fuel.

Alternatively, even if the ^{238}U cross section is only 0.014 b, one can obtain a breeder reaction stage by modestly increasing f_5. Case *C* has $\sigma_f = 0.014$ b but uses an enrichment of $f_5 = 0.20$ instead of 0.14. The results in Fig. 1 panel (c) show two well-separated reaction stages and the fission of a large fraction of available nuclei similar to Case *B*.

We have assumed that the fission fragments are essentially inert. Although there may not be time for β decay, the fission fragments could capture neutrons. Many fission fragments have (n, γ) cross sections for 1-MeV neutrons of order ≈ 0.01 b [13]. Therefore, to explore this we simply assign all fission fragments a 0.01 b capture cross section for Case *D*, see Table III. This case is otherwise identical to Case *B*. Note that we are not keeping track of the identity of each fission fragment so when a fragment captures a neutron its identity does not change. Therefore, neutron capture on fission fragments simply acts as a neutron sink.

Figure 1 panel (d) shows that capture on fission fragments somewhat reduces the abundance of neutrons. Indeed Case *B* has a finite abundance of neutrons remaining. This artificial result reflects the limitations of the reaction network. In Case *D* all neutrons are eventually captured. The reduction in neutrons slows the production of fission fragments somewhat. However, by the time the reaction is over, the total number of fission fragments and, therefore, the total fission energy released are only slightly smaller in Case *D* with capture than originally in Case *B*.

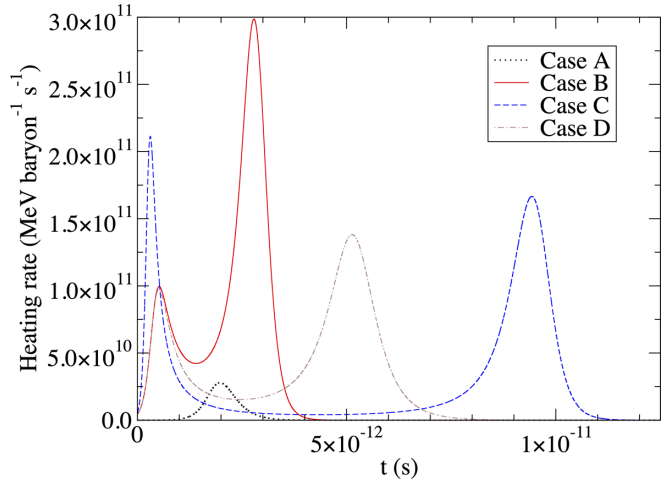

FIG. 2. Heating rate per baryon $\dot{S}(t)$ versus time for the four cases in Table III.

B. Heat release and final temperature

The heating rate for the different scenarios is shown in Fig. 2, and the total heating is plotted in Fig. 3 and listed in Table III. The final temperature is plotted in Fig. 4 for a range of f_5 values. There is a minimum value of f_5 for the system to be critical. Below this value there is almost no fission heating and T_f is small. Next there is a modest range of f_5 values where significant ^{235}U fissions but little ^{238}U or Th fissions. Here T_f is between ≈1 and 2×10^9 K. Finally there is a sharp transition when there are enough neutrons for an essentially

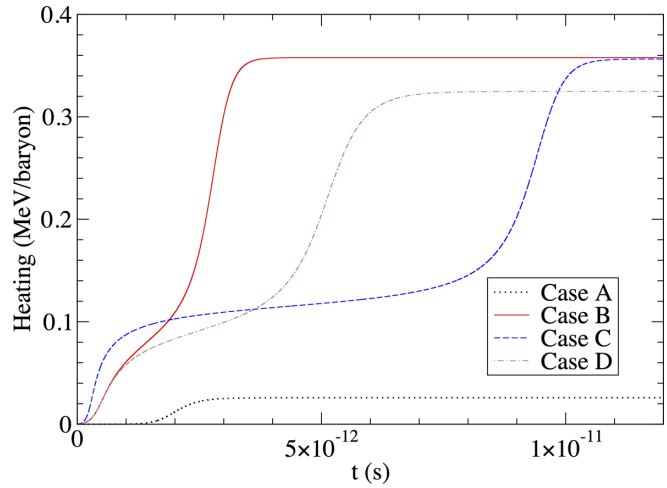

FIG. 3. Total fission heating per baryon $S(t)$ versus time for the four cases in Table III.

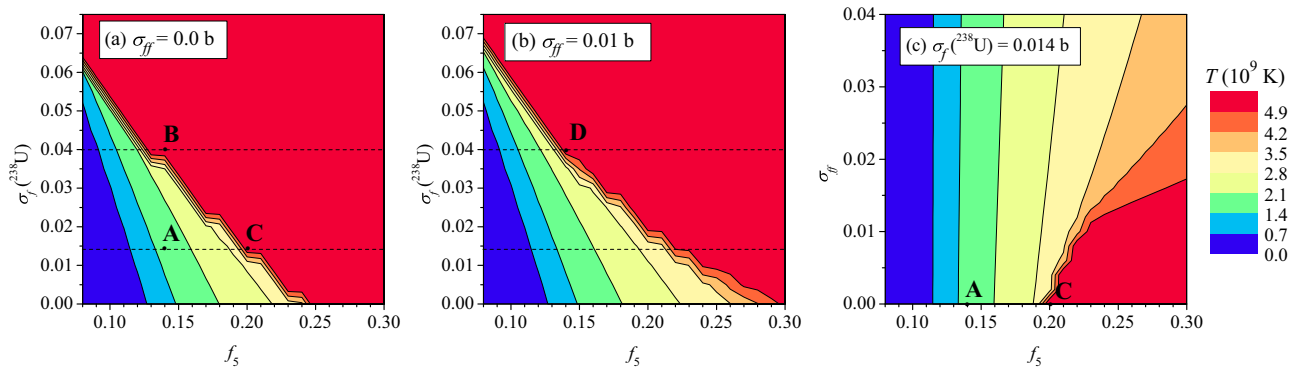

FIG. 4. Final temperature as a function of f_5 and $\sigma_f(^{238}\mathrm{U})$ using constant $\sigma_{\mathrm{ff}} = 0$ (left) and 0.01 b (center). The right panel shows the final temperature as a function of f_5 and σ_{ff} at constant $\sigma_f(^{238}\mathrm{U}) = 0.014$ b. We compute 368 networks in (a) and (b) and 483 networks in (c); the jagged regions are an artifact of the finite resolution of the grid. Scenarios *A*–*D* from Table III are indicated in the panels. The red region approximately reaches carbon ignition [16].

complete breeder reaction stage that fissions most of the U and 58% of the Th.

Note that the breeder reaction stage leads to a large total energy release of ≈0.36 MeV/nucleon as listed in Table III; this leads to $T_f \approx 6 \times 10^9$ K. As the ^{238}U fission cross section increases, the necessary f_5 for the breeder reaction decreases. In general, the breeder reaction uses all available fuel resulting in a nearly complete burn.

According to Fig. 6 of Timmes and Woosley [16] a final temperature of $T_f \approx 6 \times 10^9$ K for a 5-mg mass may be hot enough to ignite carbon burning. However, hydrodynamical simulations should be performed to explicitly verify that the energy release S heats the system enough to start carbon burning, which we reserve for future work. We note that the presence of Pb in Table I significantly increases the heat capacity without increasing the fission energy released. If the amount of Pb were less (or absent) the system would reach higher temperatures.

C. Cross section and enrichment sensitivity

To explore sensitivity to input parameters we have performed large numbers of reaction network simulations. The frames in Fig. 4 were prepared by computing a grid of networks to find the final temperature as a function of f_5, $\sigma_f(^{238}\mathrm{U})$, and σ_{ff}. In Figs. 4(a) and 4(b) we compare the final temperature when excluding neutron captures on the fission fragments (i.e., $\sigma_{\mathrm{ff}} = 0.0$ b) and assuming a modest $\sigma_{\mathrm{ff}} = 0.01$ b as an average neutron-capture cross section, respectively. The grid is computed between $f_5 = 0.08$ and $f_5 = 0.30$ at a resolution of $\Delta f_5 = 0.01$, and between $\sigma_f(^{238}\mathrm{U}) = 0.00$ and 0.075 b with a resolution of $\Delta\sigma_f(^{238}\mathrm{U}) = 0.005$ b, for a total of 368 network calculations. The cases *A*–*D* from Table III are marked in Fig. 4.

In Fig. 4(a), where no neutron captures occur on the fission fragments, there is a sharp transition between the incomplete burn or "fizzle" behavior at low f_5 and the complete burn at high f_5 where the final temperature is $T_f \gtrsim 5 \times 10^9$ K. For enrichments $f_5 \lesssim 0.25$ the transition between incomplete/complete burns depends on $\sigma_f(^{238}\mathrm{U})$, requiring larger $\sigma_f(^{238}\mathrm{U})$ for a complete burn at lower enrichment f_5. For enrichments $f_5 \gtrsim 0.25$ a nonzero $\sigma_f(^{238}\mathrm{U})$ always results in a complete burn. In Fig. 4(b) the fission fragments act as a neutron sink with a cross section of $\sigma_{\mathrm{ff}} = 0.01$ b. In this case, the burning transition shifts to higher f_5. However, at nonzero $\sigma_f(^{238}\mathrm{U})$ we still find a robust burn of the ^{238}U and Th.

In Fig. 4(c) we explore the sensitivity to the fission fragments as a neutron sink assuming constant $\sigma_f(^{238}\mathrm{U}) = 0.014$ b. We use a resolution of $\Delta\sigma_{\mathrm{ff}} = 0.002$ b; the resolution in f_5 is the same as above for a total of 483 networks. For low values of σ_{ff} [i.e., $\sigma_{\mathrm{ff}} \lesssim \sigma_f(^{238}\mathrm{U})$], we find that complete burns are still readily achieved for $f_5 \gtrsim 0.20$. It is only at $\sigma_{\mathrm{ff}} \gtrsim \sigma_f(^{238}\mathrm{U})$ that the fission fragments begin to "outcompete" the ^{238}U for neutrons and quench the burning. Thus, even with some degree of "poisoning" due to neutron captures onto fission fragments, or other impurities, the system may still undergo a complete burn so long as $\sigma_f(^{238}\mathrm{U})$ (and f_5) is sufficiently high.

In Fig. 5 we show the total percentage of Th and U that fissions in the grid of networks computed in Fig. 4. It is clear that barely any Th (top) burns in networks that fizzle at low f_5 [Fig. 5(a)], and that the conditions required for a complete burn Th burning have a sharp transition. Neutron captures on the fission fragments can suppress the total Th fraction that fission [Figs. 5(b) and 5(c)], and the sharp turn on is shifted to slightly greater f_5. When we compare to the U fraction that burns (bottom) in the networks that fizzle, we see that most of the ^{235}U burns, but barely more than f_5, so the heating is largely due to a ^{235}U burning which then stalls before igniting the breeder stage. We conclude that the final temperatures observed in Fig. 4 can be explained by a steady increase in ^{235}U burning with increasing f_5 in the fizzling regime with complete burns achieved after a very sharp turn on which burns the Th and ^{238}U in a breeder stage.

V. DISCUSSION

In this section we discuss limitations in our reaction network and then carbon ignition.

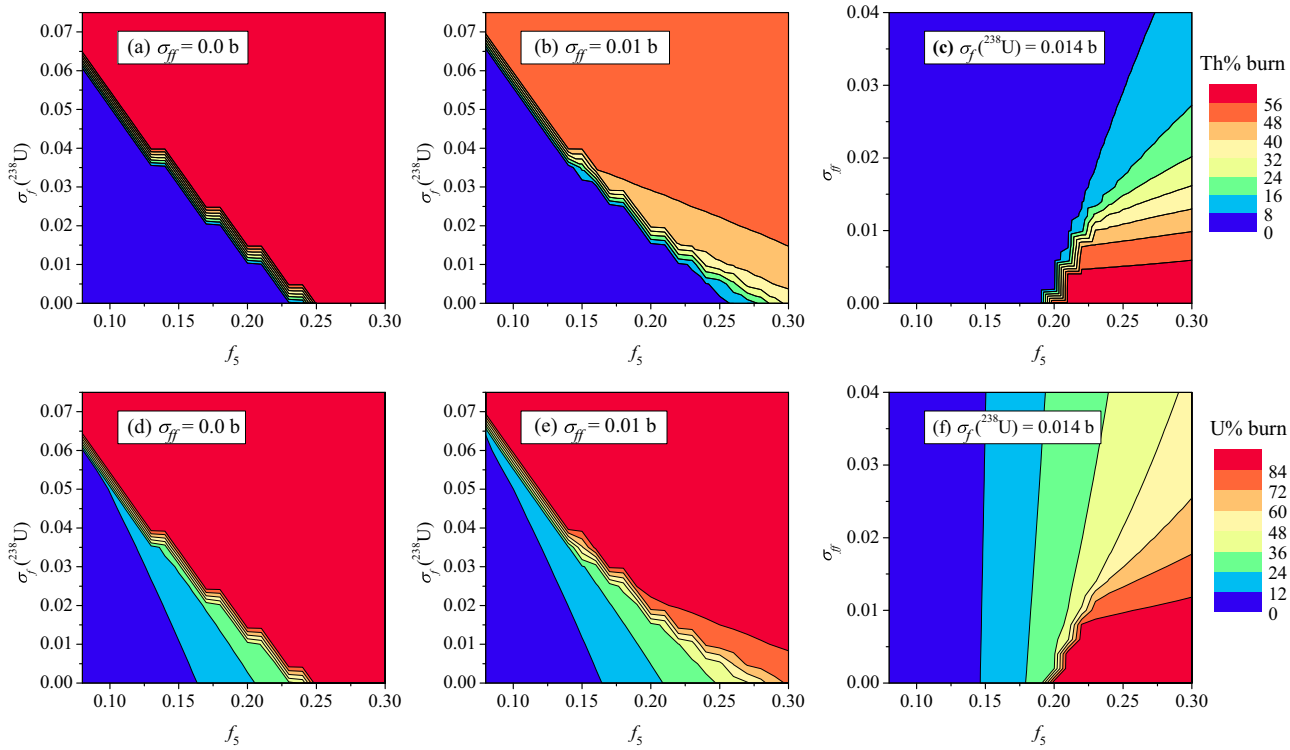

FIG. 5. Percentage of Th that fissions (top) and total fraction of U that fissions (bottom) for the same simulations as in Fig. 4.

A. Limitations of reaction network

We now explore possible limitations in our reaction network. First we have only included (n, γ) and fission reactions. These reactions proceed very rapidly on a timescale of $\tau \approx 10^{-15}$ s and neglecting β decay and (γ, n) should be a good first approximation. We have neglected $(n, 2n)$ reactions because these should be unimportant except at high neutron energies above 1 MeV. In future work we will examine temperature-dependent cross sections and any new reaction pathways that may result.

Our reaction network assumes 1-MeV neutrons. This is a reasonable first approximation to the fission spectrum as long as the amount of light nuclei, such as C or O is small. If light nuclei are present, then nuclear recoil following elastic scattering will reduce the neutron energies. In future work we will explore sensitivity of the reaction network to the neutron spectrum.

Our reaction network is somewhat incomplete and does not include reactions for very neutron-rich Th or U isotopes. For U we include reactions on isotopes up to ^{241}U. The omission of reactions on ^{242}U or heavier isotopes is not expected to be important because most of the U fissions and only a tiny fraction captures enough neutrons to reach ^{242}U.

For Th we only include reactions on ^{232}Th and ^{233}Th. For Cases *B–D* a significant fraction of the original Th is converted to ^{234}Th (which is stable in our network). Including reactions on heavier Th isotopes could lead to the fission of more Th. In particular, the neutron-induced fission of ^{235}Th could be a significant addition to our reaction network. There may not be data for this neutron-rich isotope, however, and further progress using our reaction network likely will require theoretical rates for very neutron-rich isotopes.

We assumed a constant baryon density in Sec. III Eqs. (2)–(4). In reality, the system will expand slightly because of the large fission energy release. However, this decrease in density is only about 25% because the electrons are degenerate [11]. This will slightly slow down the rate of all neutron reactions and, therefore, the chain reaction will take slightly longer to complete.

We have neglected cooling from heat conduction and neutrino emission. This should be a good approximation during the fission reaction because the reaction rates are so high. The fission heating rate in Fig. 2 is consistent with the estimated rate in Ref. [11]. The rate of cooling from heat conduction via the large thermal conductivity of the degenerate electrons is estimated in Ref. [11] to be two to three orders of magnitude lower than the heating rate in Fig. 2. Therefore, heat conduction is unimportant during the fission reaction.

B. Carbon ignition and explosive yield

We now consider carbon ignition. After the fission chain reaction, the system may be so hot that self-propagating thermonuclear carbon burning is initiated. Such a scenario is unstudied, and future hydrodynamical simulations will be needed. In the meantime, however, we can examine the fission scenario through analogy with terrestrial nuclear weapons.

First for context, we discuss ignition of hydrogen isotopes in a terrestrial nuclear weapon. The classical super was the original idea to use heat from an atomic bomb to start fusion in a deuterium and tritium mixture. It is said that losses from thermal radiation will help quench thermonuclear fusion in the classical super. Instead, radiation implosion can be used to compress the hydrogen fuel first. This compression increases the energy density from hydrogen fusion without increasing the radiation losses. In a WD, the carbon fuel is already at a very high density. Therefore radiation losses are likely unimportant, and our system may avoid this problem with the classical super. Because of the high initial density there may be no need for radiation implosion to compress the system further.

It is interesting to compare the explosive yields in our system to those of nuclear weapons. Previously we had estimated the initial mass of the uranium-rich crystal to be about 5 mg [10,11]. In Cases *B–D* we find a significant fraction of the U and Th in this 5-mg mass fissions. This will release energy equivalent to about 50 kg of TNT. The yield is much lower than the approximately 15 kiloton yield of the first atomic bombs because the 5-mg mass of our system is much less than the multikilogram core masses of conventional fission weapons.Note that the efficiency of our system may be much higher with nearly all of the U and Th fissioning, compared to the few percentage efficiency of an atomic bomb. Nevertheless, because the mass and critical mass are so much smaller, our fission yield is almost 10^6 times smaller. Therefore, if carbon burning is not initiated, the fission chain reaction may have very little effect on the star.

The situation is dramatically different if carbon burning is initiated. The thermonuclear burning of a significant fraction of C in a WD will release energy comparable to a SN Ia. This corresponds to an explosive yield of almost 10^{29} megatons (MT)! Thus, we propose using a 50-kg yield fission *primary* to ignite a 10^{29}-MT fusion *secondary*.

The temperature required for carbon ignition depends on the ignition scenario including the system size, density, and ignition timescale. Our system has a density near 10^8 g cm^{-3} and a total mass of order 5 mg. The original work of Timmes and Woosley may be the most directly relevant previous calculation of ignition temperature for our conditions [16]. They consider ignition in a C/O liquid where they instantaneously replace a small mass of C/O by carbon-burning ashes and assume the temperature of this ash has been raised to T_i. They find an ignition temperature of $T_i \approx 5 \times 10^9$ K. If the final temperature $T_f > T_i$ a flame may propagate in the surrounding C/O liquid. If $T_f < T_i$ the system will cool via heat conduction without initiating carbon burning. This ignition temperature of 5×10^9 K should be verified with future hydrodynamic simulations.

VI. CONCLUSIONS

In this paper we have performed novel reaction network simulations of fission chain reactions in a cooling WD. The first solids to form when material in a WD just starts to crystallize are expected to be U and Th rich because of their high charges. These solids may support a fission chain reaction if the uranium enrichment f_5 is high enough > 0.12.

We find that the reaction proceeds very quickly (within $\approx 10^{-11}$ s) because the density is high and the neutron cross sections are large. In general, the reaction proceeds in two stages. In the first stage neutrons from ^{235}U fission transform or breed some ^{238}U and ^{232}Th nuclei into more easily fissionable ^{239}U and ^{233}Th. In the second, or breeder reaction, stage most of the original U and a significant fraction of the Th fission are fissionable. These reaction stages release ≈ 0.36 MeV/nucleon and raise the final temperature to $T_f \approx 6 \times 10^9$ K. This is important input for our thermal diffusion simulations where we find that carbon ignition is likely at high densities [12].

ACKNOWLEDGMENTS

We thank E. Booker, C. Deliyannis, E. Holmbeck, W. Misch, M. Mumpower, W. Nazarewicz, C. Pilachowski, T. Plewa, and R. Surman for helpful discussions. The work of C.J.H. was performed, in part, at the Aspen Center for Physics, which is supported by National Science Foundation Grant No. PHY-1607611. This research was supported, in part, by the U.S. Department of Energy Office of Science Office of Nuclear Physics Grants No. DE-FG02-87ER40365 and No. DE-SC0018083 (NUCLEI SCIDAC).

[1] T. M. C. Abbott, S. Allam, P. Andersen, C. Angus, J. Asorey, A. Avelino, S. Avila, B. A. Bassett, K. Bechtol, G. M. Bernstein *et al.*, Astrophys. J. Lett. **872**, L30 (2019).
[2] D. A. Howell, Nat. Commun. **2**, 350 (2011).
[3] M. Sullivan, Type ia supernovae and cosmology, in *Lectures on Cosmology: Accelerated Expansion of the Universe*, edited by G. Wolschin (Springer, Berlin/Heidelberg, 2010), pp. 59–97.
[4] A. G. Riess, L. M. Macri, S. L. Hoffmann, D. Scolnic, S. Casertano, A. V. Filippenko, B. E. Tucker, M. J. Reid, D. O. Jones, J. M. Silverman, R. Chornock, P. Challis, W. Yuan, P. J. Brown, and R. J. Foley, Astrophys. J. **826**, 56 (2016).
[5] A. G. Riess, S. Casertano, W. Yuan, J. B. Bowers, L. Macri, J. C. Zinn, and D. Scolnic, Astrophys. J. Lett. **908**, L6 (2021).
[6] E. Di Valentino, O. Mena, S. Pan, L. Visinelli, W. Yang, A. Melchiorri, D. F. Mota, A. G. Riess, and J. Silk, Class. Quantum Grav. **38**, 153001 (2021).
[7] B. Wang and Z. Han, New Astron. Rev. **56**, 122 (2012).
[8] W. Hillebrandt, M. Kromer, F. K. Röpke, and A. J. Ruiter, Front. Phys. **8**, 116 (2013).
[9] P. Ruiz-Lapuente, New Astron. Rev **62-63**, 15 (2014).
[10] C. J. Horowitz and M. E. Caplan, Phys. Rev. Lett. **126**, 131101 (2021).
[11] C. J. Horowitz and M. E. Caplan, arXiv:2107.03568.

[12] C. J. Horowitz, ApJL **935**, L2 (2022).
[13] National Nuclear Data Center is sponsored by the Office of Nuclear Physics, Office of Science, U.S. Department of Energy and can be accessed at http://www.nndc.bnl.gov.
[14] J. Lippuner and L. F. Roberts, Astrophys. J., Suppl. Ser. **233**, 18 (2017).
[15] Y. Zhu and J. C. Pei, Phys. Rev. C **94**, 024329 (2016).
[16] F. X. Timmes and S. E. Woosley, Astrophys. J. **396**, 649 (1992).